Eur J Med Chem (1996) 31, 319–330

Short communication

Acetylcholine release enhancers related to linopirdine: a structure–activity relationship study. II*

WW Wilkerson, RA Earl, JC Calabrese, S Drummond, CA Teleha, ME Voss, R Zaczek

DuPont Merck Pharmaceutical Company, Chemical and Physical Sciences, Experimental Station E500/3203, PO Box 80500, Wilmington, DE 19880-0500, USA

(Received 28 August 1995; accepted 6 December 1995)

Summary — Several series of α,α-disubstituted polycyclic compounds were found to enhance the stimulus-induced release of neurotransmitters, especially acetylcholine, in brain slices. This work resulted in the identification of linopirdine [3,3-bis(4-pyridinylmethyl)-1,3-dihydro-1-phenyl-2*H*-indol-2-one] **1a** which was tested clinically for the treatment of Alzheimer's disease. The structure–activity relationship (SAR) results suggest that the potency of the series was dependent on the nature of the pendent groups (R), the distance geometry produced by the pendant groups, and the hydrogen-bonding property of the core group.

acetylcholine release enhancer / linopirdine / cognition / Alzheimer's disease / structure–activity relationship (SAR)

Introduction

Alzheimer's disease (AD) is a neurodegenerative disease of the aged, generally being diagnosed after the age of 56, and affecting up to 10% of the population over the age of 65. The disease affects 30% or more of the population over the age of 80. In the developed world, AD is the fourth major cause of death after cardiovascular disease, cancer, and stroke. With an increase in life expectancy due to medical advances in treating the above diseases, the number of AD patients is anticipated to increase dramatically. Early in the study of AD it was discovered from the post mortem findings that significant deficits existed in the synthesis and amount of the neurotransmitter acetylcholine (AcCh) in the brains of AD patients compared to that found in the normal aged brain, and that these deficits were related to cognitive impairment [2]. These observations resulted in our research efforts to find compounds capable of enhancing the stimulus-induced release of this neurotransmitter in the brain of AD patients.

Recently, we reported on the synthesis and structure–activity relationship (SAR) associated with a series of 3-substituted, 3-(4-pyridinylmethyl)-1,3-dihydro-1-phenyl-2H-indol-2-ones (**I**) acetylcholine (AcCh) release enhancers [3]. These compounds were synthesized and investigated because of our interest in the AcCh release enhancer linopirdine (**1a**) which has been discussed previously [4–16]. Our results suggest that the ability of these compounds to enhance the release of AcCh from brain slices could be correlated with the distance between the pyridyl nitrogen of one pendant group (R1) and the hydrogen-bond-accepting (HBA) moiety of the second pendant group (R2) [3]. This study was conducted, largely after the identification of **1a**, in an attempt to confirm the importance of the distance geometry of the pendant groups to activity, and to investigate the contribution to activity associated with the 'core' group. This study, in conjunction with the previous results, was used to develop a template for future drug design.

Synthesis, structures, and biology

The compounds in this report are composed of two components: two pendant groups R-CH_2 and a core group to which the pendant groups are attached (fig 1). Detailed studies on the synthesis and characterization of the compounds in this report have previously been reported [5, 10, 17–20]. All the compounds in this report can be synthesized as illustrated in scheme 1 and exemplified by the synthesis of **2a**. Structures and physicochemical data are listed in table I.

*Portions of this report were presented at the *12th International Symposium on Medicinal Chemistry* [1].

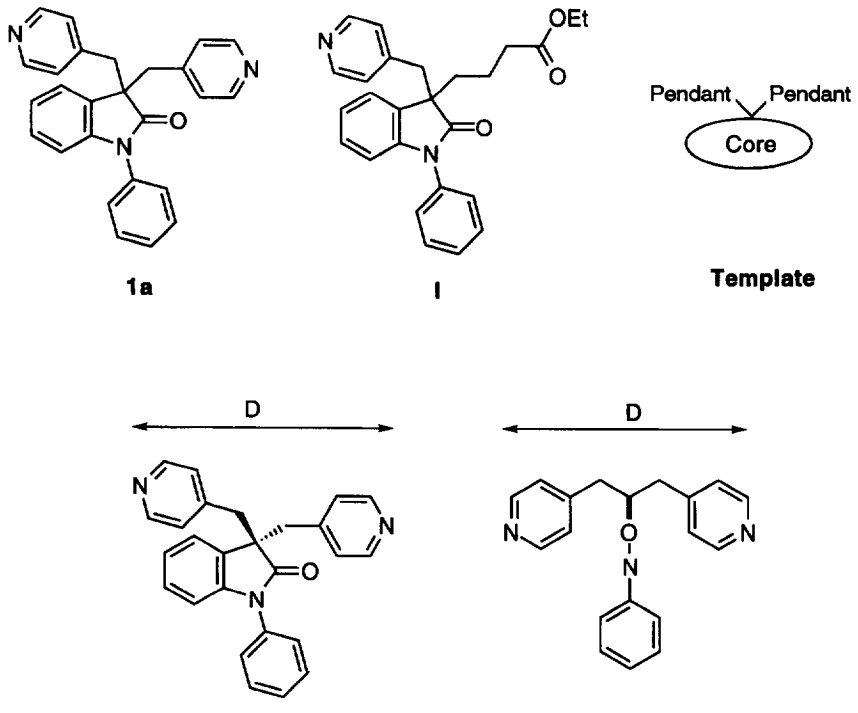

Fig 1. AcCh release enhancers.

The assay for the stimulus-induced release of AcCh release was a modification of the procedure described by Nicholson et al [12] as reported by Wilkerson et al [3]. The results are reported as the EC_{50} (μM) 'amount of compound required to produce 50% of AcCh release caused by 10 μM of a standard (**1a**)' [3]. On the basis of the results from a large number of compounds, it has been determined that the standard error (se) for the method is ≤13%. Also listed in table I is the normalized percentage release of AcCh caused by 10 μM of each compound defined by:

Normalized AcCh release =

$$\left[\frac{\text{(compound \% release at 10 μM)} - \text{control}}{\text{(standard \% release at 10 μM)} - \text{control}}\right] \times 100$$

where control is the untreated tissue and the standard was linopirdine dihydrochloride (**I**). The structures and EC_{50} for AcCh release are listed in table I.

Computer systems and software

Graphs and statistical presentations were obtained using CA–Cricket Graph III v1.5 by Computer Associates International Inc, Islandia, NY, and JMP v3.0.2 by SAS Institute, Cary, NC, USA. Computer-generated Clog *P* and CMR were obtained using MedChem Software v3.0, Pomona College, Claremont, CA, USA in conjunction with a Power Macintosh 7100/80. Substituents constants were taken from Hansch and Leo [21]. Distance geometry (*D*) was obtained on energy-minimized structures using CSC Chem3D Plus v3.1 by Cambridge Scientific Computing Inc, Cambridge, MA, USA.

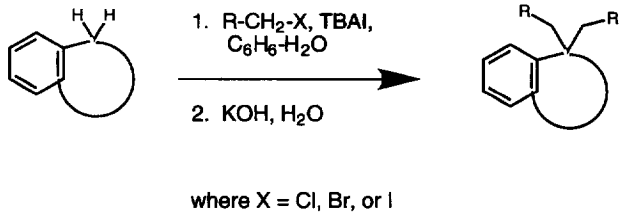

Scheme 1. General synthetic approach to the α,α-disubstituted aromatic and heteroaromatic systems useful as acetylcholine-release enhancers.

Table I. Structures and enhancement of K^+-stimulated AcCh release activity for compounds **1–17**.

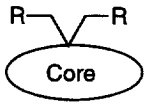

Compound	*R*	*Core*	*Mp (°C)*	*Formula*	*EC_{50} (μM)** (normalized % release at 10 μM)*
1a	 4-Pyr	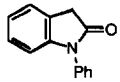 OX	183–185	$C_{26}H_{21}N_3O$	4.3 (127)
1b	 4-Pym	OX	152–154	$C_{24}H_{19}N_5O$	7.6 (67)
1c	 3-Pyr HCl	OX	156–157	$C_{26}H_{23}N_3OCl_2$	14.0 (36)
1d	 2-Pyr HCl	OX	250–251	$C_{26}H_{23}N_3OCl_2$	25.8 (19)
2a	4-Pyr	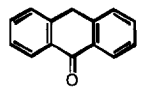 AN	228–231	$C_{26}H_{20}N_2O$	0.4 (216)
2b	4-Pym	AN	195–198	$C_{24}H_{18}N_4O$	4.4 (1.03)
2c	3-Pyr	AN	189–191	$C_{26}H_{20}N_2O$	11.5 (57)
2d	2-Pyr	AN	199–200	$C_{26}H_{20}N_2O$	26.9 (17)
2e	 Ph	AN	219–221	$C_{28}H_{22}O$	200 0 (~ 1)
3	4-Pyr HCl	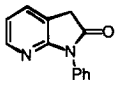 AZO	210–212	$C_{25}H_{22}N_4OCl_2$	4.4 (102)
4	4-Pyr HCl	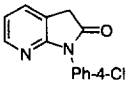 CAZO	137 dec	$C_{25}H_{21}N_4OCl_3$	5.0 (110)
5a	4-Pyr	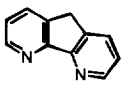 4,5-DAF	> 300	$C_{23}H_{18}N_4$	6.3 (86)
5b	4-Pyr	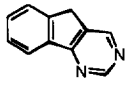 2,4-DAF	172–175	$C_{23}H_{18}N_4$	7.4 (77)

Table I. *Continued.*

Compound	*R*	*Core*	*Mp (°C)*	*Formula*	*EC_{50} (μM)** (normalized % release at 10 μM)*
5c	4-Pyr	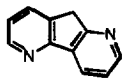	140–141	$C_{23}H_{18}N_4$	17.6 (36)
5d	4-Pyr	1,5-DAF 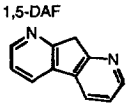	244–247	$C_{23}H_{18}N_4$	40.3 (1)
5e	4-Pyr	1,8-DAF 	199–202	$C_{23}H_{18}N_4$	8.8 (71)
6	4-Pyr HCl	1,2-DAF 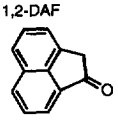	255 dec	$C_{24}H_{20}N_2OCl_2$	6.2 (86)
7a	4-Pyr	ACE 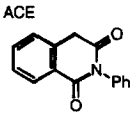	> 270	$C_{27}H_{21}N_3O_2$	7.5 (77)
7b	4-Pyr	H-PPI 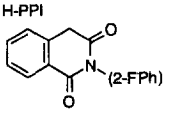	256–259	$C_{27}H_{20}FN_3O_4$	2.0 (139)
7c	4-Pyr	2-F-PPI 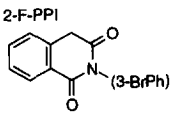	236–238	$C_{27}H_{20}BrN_3O_4$	2.4 (132)
7d	4-Pyr	3-Br-PPI 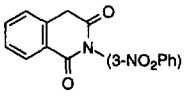	212–214	$C_{27}H_{20}N_4O_4$	5.2 (96)
7e	4-Pyr	3-NO_2-PPI 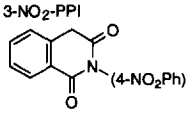	230–232	$C_{27}H_{20}N_4O_4$	3.2 (118)
8	4-Pyr	4-NO_2-PPI 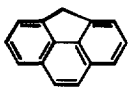	200–202	$C_{27}H_{20}N_2$	7.0 (81)
9	4-Pyr	CPPA 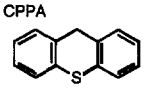	201–203	$C_{25}H_{20}N_2S$	10.1 (63)
10	4-Pyr HCl	TXT 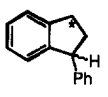	> 210	$C_{27}H_{26}N_2Cl_2$	10.8 (60)

Table I. *Continued.*

Compound	*R*	*Core*	*Mp (°C)*	*Formula*	*EC_{50} (μM)** (normalized % release at 10 μM)*
11	4-Pyr	PID 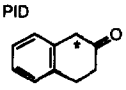	111–112	$C_{22}H_{20}N_2O$	16.1 (41)
12	4-Pyr	TTL 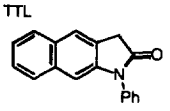 PNL	209–211	$C_{30}H_{23}N_3O$	16.8 (39)
13	4-Pyr	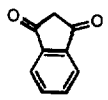	184–186	$C_{21}H_{16}N_2O_2$	22.6 (24)
14	4-Pyr	IDD 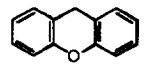	212–213	$C_{25}H_{20}N_2O$	5.7 (90)
15a	4-Pyr	XT 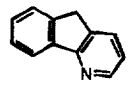 4-AF	163–164	$C_{24}H_{19}N_3$	2.0 (138)
15b	4-Pyr	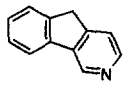	182–183	$C_{24}H_{19}N_3$	5.0 (97)
15c	4-Pyr	3-AF 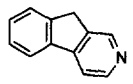	142–143	$C_{24}H_{19}N_3$	8.8 (71)
15d	4-Pyr	2-AF 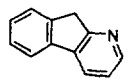	205–206	$C_{24}H_{19}N_3$	14.5 (47)
16a	4-Pyr HCl	1-AF 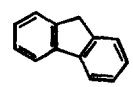 FL	321–323	$C_{25}H_{22}N_2Cl_2$	6.0 (88)
16b	Ph	FL	oil	$C_{27}H_{22}$	201.0 (~ 1)
17	4-Pyr HCl	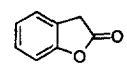 CMN	269–270	$C_{20}H_{18}N_2O_2Cl_2$	14.5 (46)

*Point of attachment; **Se < ± 13%.

X-ray studies

X-ray crystallography structures were obtained on an Enraf–Nonius diffractometer for selected compounds in this study (fig 2, 3). The X-ray study confirmed the expected structure of the indolin-2-one **1a** with two pyridylmethyl groups attached to the lactam ring. In this conformation, the pyridylmethyl groups are rotated to symmetrically flank the lactam ring. X-ray analysis of **2a** showed that the angle between the two pyridyl rings is 119.2°. The distance between the two pyridyl nitrogen atoms is 10.31 Å and may be compared to 9.52 Å for **1a**. The distance between the carbonyl oxygen, O1, and N19 is 6.44 Å, and the distance between O19 and N26 is 5.86 Å. There is a strong interaction between the water molecule and the pyridyl nitrogen atoms. Relevant crystal data and method information are shown in table II, and all X-ray data are available upon request. The X-ray structure of **2e** has been published [22], and the conformation was found to be not significantly different from that of **2a**.

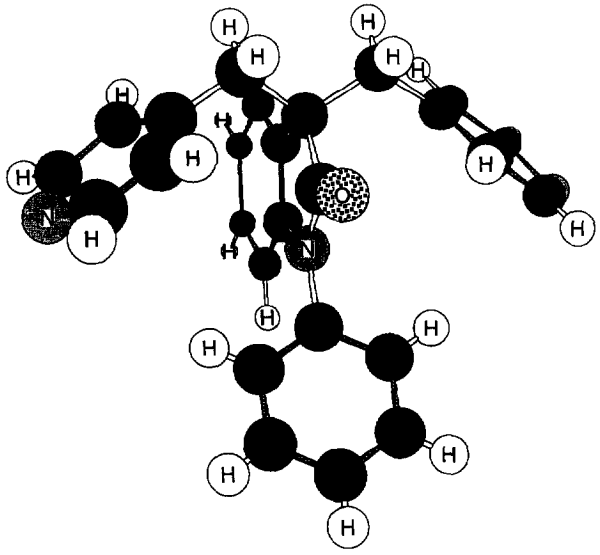

Fig 2. X-ray crystal structure of **1a**.

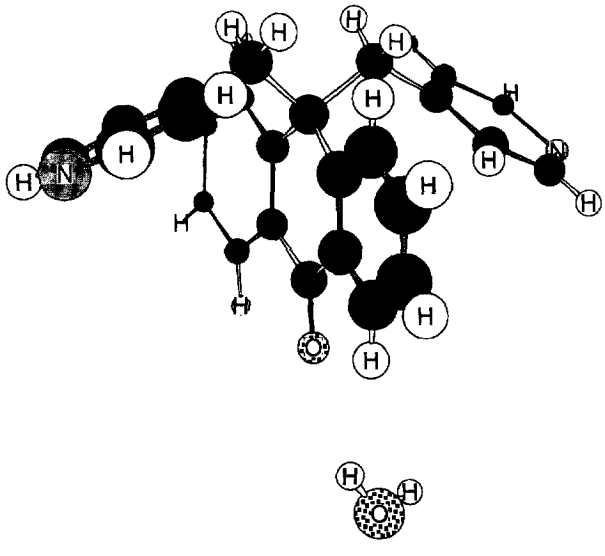

Fig 3. X-ray crystal structure of **2a**.

The computer-minimized structures for all the compounds in this study assumed the 'gull wing' conformation as shown in figures 4 and 5. This conformation is not significantly different from that observed from X-ray crystallography (**1a**, **2a**, **2e** and **5a**). Because we felt that the distance (D) between the nitrogen atoms (N → N) of the pendant groups was important to activity, we compared the X-ray distances with those obtained from the computer generated structures (see table III). The largest difference in distance was observed for **2a** ($D_{\text{X-ray}} - D_{\text{computer}} = \Delta D$ = +0.56 Å), and **1a** and **5a** had differences of –0.23 Å and +0.22 Å, respectively. Because ΔD did not parallel activity, we felt confident in using the minimized structure distance data for our SAR–QSAR studies.

Discussion

Pendant groups

Table IV shows data on a representative series of substituted cores where the core was *N*-phenyloxindole (**1a–d**) and anthrone (**2a–e**). The only structural variable for these two sets of cores was the nature of the R-moiety. An inspection of these data showed the following concerning AcCh releasing activity: **1a** (4-Pyr-CH_2) > **1b** (4-Pym-CH_2) > **1c** (3-Pyr-CH_2) > **1d** (2-Pyr-CH_2). The same pattern of activity was observed for the anthrones: **2a** > **2b** > **2c** > **2d**. Except for the 4-pyrimidines **1b** and **2b**, these R-groups have the same Clog *P* (R = 4-Pyr = 3-Pyr = 2-Pyr = 2.86), and CMR (R = 4-Pyr = 3-Pyr = 2-Pyr = 11.88), suggesting that neither of these parameters by itself was important for activity. We investigated the importance of pK_a for the series by comparing measured pK_a values for R-CH_3. Attempts to measure pK_a values for the compound series **1** and **2** were not satisfactory. The pK_a data would suggest that increasing pK_a results in increased activity. However, the introduction of the data for the 4-Pym compounds destroyed this relationship, suggesting that pK_a of the R-group was also not important, in itself, to activity.

Table II. X-ray crystallography data for AcCh release enhancers **1a** and **2a**.

	1a	*2a*
Formula; MW	$C_{26}H_{21}N_3O$; 391.77	$C_{26}H_{20}N_2OH_2O$; 394.47
Solvent system	EtOAc	EtOH/EtOAc
Crystal system	plate	cube
Space group	$P2_1/n$ (No. 14)	P21/n (No. 14)
Lattice constant *a* (Å)	10.151 (4)	9.154 (4)
b (Å)	16.902 (6)	12.103 (3)
c (Å)	12.191 (5)	19.031 (7)
β (deg)	91.05 (3)	99.85 (2)
T °C	–70	–70
V (Å^3)	2091.3	2078.2
D_{calc} (g cm^{-1})	1.243	1.261
μ for Mo Kα (cm^{-1})	0.72	0.75
Crystal size (mm^3)	0.027	0.120
	(0.15 x 0.45 x 0.40)	(0.49 x 0.50 x 0.49)
Color, habit	colorless	faint amber
Obs 2 θ range (deg)	4–50	2.2–4.8
No reflections obs as I > 3 σ (I)	1854	2112
Used for structure determination	1854	2112
Symmetry equiv	177	105
Refinement by	full-matrix least-squares on F	full-matrix least-squares on F
Final R value	0.043	0.041
Refined atoms	anisotropic all non-H atoms	all non-H atoms
	isotropic H	H
Diffractometer	Enraf–Nonius CAD4	Enraf–Nonius CAD4

Regression analysis produced equations (1a,b) where *D* represents the distance between the heteroatoms of the two pendant groups (fig 1) for the molecules that have been subjected to energy minimization:

$$-\log (EC_{50})_{OX} = 0.18\ (\pm 0.05)\ D - 2.55\ (\pm 0.41) \quad (1a)$$
$n = 4$; $r = 0.937$; se = 0.143; $F = 14.478$; Prob > $F = 0.063$

$$-\log (EC_{50})_{OX\&AN} = 0.33\ (\pm 0.10)\ D + 0.18\ (\pm 0.13)\ \text{Clog}\ P - 4.18\ (\pm 1.08) \quad (1b)$$
$n = 8$; $r = 0.819$; se = 0.400; $F = 5.089$; Prob > $F = 0.062$

We had observed that the compounds with a heteroatom in the pendant group were always more active

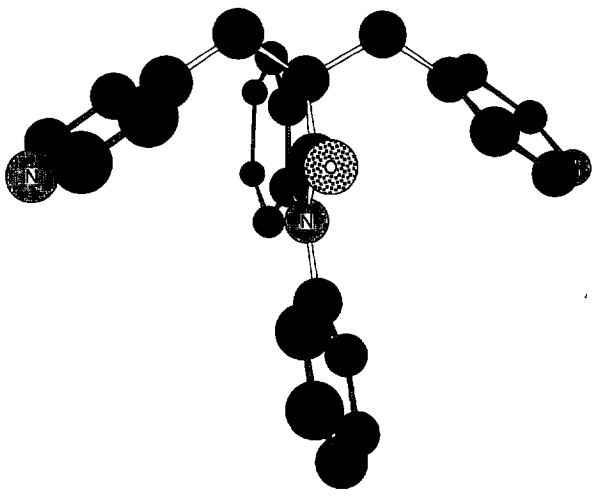

Fig 4. Chem3D Plus™ structure of the conformer of minimum energy for **1a**.

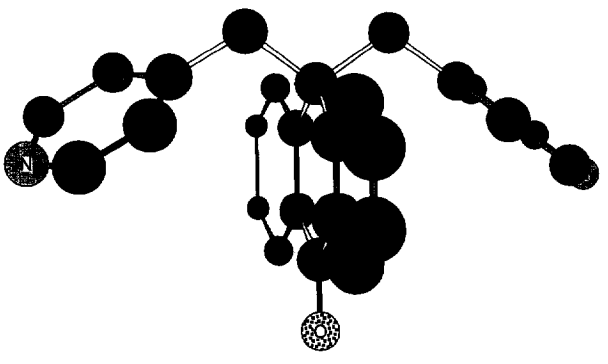

Fig 5. Chem3D Plus™ structure of the conformer of minimum energy for **2a**.

Table III. X-ray and computer modeling data comparisons for **1a** and **2a**.

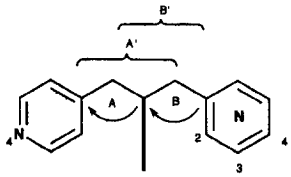

Compound	*Angle A (°)*	*Angle B (°)*	*Distance N → N, Å*	*Dihedral angle A' (°)*	*Dihedral angle B' (°)*	*EC_{50} (μM)*
1a						4.3
X-ray	114.8	115.3	9.52			
Computer	113.8	120.0	9.75	−176.9	162.5	
2a						
X-ray	115.8	116.5	10.31			
Computer	112.2	111.9	9.75	−173.4	169.2	

Table IV. Data for SAR studies on the pendant groups **R**.

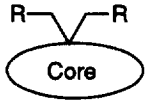

Compound	*R*	*Core*	*−log (EC_{50}) μM*	*D (Å)*	*Clog P*	*CMR*	*pKa R-CH_3 ±0.5%*
1a	4-Pyr	OX	−0.633	9.75	2.86	11.88	6.01
1b	4-Pym	OX	−0.881	9.57	0.61	11.40	2.03
1c	3-Pyr	OX	−1.146	8.35	2.86	11.88	5.63
1d	2-Pyr	OX	−1.412	6.00	2.86	11.88	5.94
2a	4-Pyr	AN	0.398	9.75	4.15	11.51	6.01
2b	4-Pym	AN	−0.643	9.62	1.90	11.09	2.03
2c	3-Pyr	AN	−1.061	8.71	4.15	11.51	5.63
2d	2-Pyr	AN	−1.430	6.33	4.15	11.51	5.94
2e	Ph	AN	−2.301	na	7.10	11.94	

nc = not calculated; na = not applicable; no heteroatom associated with R2.

than the corresponding non-heteroatom species (**2a–d** vs **2e**), and (**16a** vs **16b**). The assumption was made that one or more of the heteroatoms was involved in hydrogen bonding (HB) with the active site, and if correct, their relative position(s) would be important. In an attempt to understand this observation, all the compounds were energy-minimized using molecular mechanics, and the distance(s) (*D*) between the heteroatoms of the two pendant groups was measured. A simple plot of EC_{50} vs *D* for **1a–d** and **2a–d** (see fig 6) showed a striking relationship between activity and *D*. Regression analysis showed a linear correlation (*r*) of 0.93 and 0.96 respectively (equations 1a,b). When the **1a–d** and **2a–d** were combined and Clog *P* was added to the regression, eq 1c resulted which suggested that *D* was a major contributor to activity and Clog *P* was a lesser contributor to activity. The best nitrogen-to-nitrogen distance for activity appeared to be 9.75 Å as represented by bis-4-Pyr nitrogen spacing. This distance is similar to that previously reported for the mixed pendant (R1-CH_2 = 4-pyridylmethyl, and R2-CH_2 = ethyl butyrate) *N*-phenyloxindoles (**I** in fig 1) [3]. We were mindful of the possibility of change correlations as a result of using such a small data set [23, 24], but we have found no exceptions to this distance geometry.

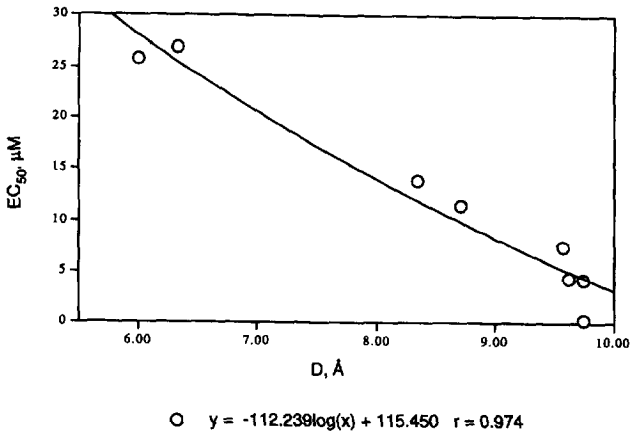

Fig 6. K^+-stimulated AcCh release-enhancing activity as a function of the distance (*D*) between the heteroatoms of the pendant groups for **1a–d** and **2a–d**.

Core groups

The AcCh releasing activity of **1a** (EC_{50} = 4.3 µM) and **2a** (EC_{50} = 0.4 µM) demonstrate that the nature of the core group affects activity (table IV). The data in table V further illustrate this observation. Structurally, the only difference between **16** and **15a–d** was the presence of a nitrogen in the core. Similarly, **16** differs from **5a–e** by the presence of two nitrogen atoms in the core. These data suggested that the presence, number, and/or position (conformation) of any heteroatoms associated with the core influenced the activity of the compound. Compounds **5a–e** all have the same CMR (10.67) and a range of Clog *P* (2.38 for **5a** to 1.96 for **5d**). Clearly these physical chemical parameters did not in themselves explain the range of observed activities (EC_{50} = 6.3 µM for **5a** to EC_{50} = 40.3 µM for **5d**). Similarly, **15a–d** all have the same CMR and Clog *P*, which further suggested that molecular dispersion (size, bulk) and lipophilicity had little influence on activity. Attempts to derive a statistically significant regression equation for –log (EC_{50}) in terms of Clog *P* and CMR have not been successful. The thioxanthene derivative **9** (EC_{50} = 10.1 ± 1.3 µM) was found to be less active than the corresponding xanthene **14** (EC_{50} = 5.7 ± 0.8 µM), and both were found to be less active than the anthrone **2a** (EC_{50} = 0.4 µM). These observations again suggested that the position and nature of the heteroatom associated with the core were important to activity. Increasing the size and/or lipophilicity of **1a** (EC_{50} = 4.3 µM) to that of **12** resulted in a loss of activity to EC_{50} = 16.8 µM. Some changes in the core would appear to have little effect on activity as illustrated by the comparisons between **1a**, **3** and **4a**, while other changes would appear to have a large influence on activity as shown with the comparison for **7a–e**. A regression analysis was conducted on the small series of homophthal-

Table V. Data for SAR-QSAR studies on the core groups.

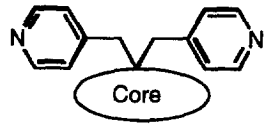

Compound	*Core*	*Clog P*	*CMR*	*EC50, µM (se < ± 13%)*
1a	OX	2.86	11.88	4.4
2a	AN	4.14	11.51	0.4
4a	CAZO	2.86	12.16	5.0
5a	4,5-DAF	2.38	10.67	6.3
6	ACE	3.45	10.69	6.2
7b	2-F-PPI	nc	12.40	2.0
8	CPPA	5.30	11.88	7.0
9	TXT	5.42	11.82	10.1
10	PID	5.48	11.94	10.8
11	TTL	2.36	9.93	16.1
12	PNL	4.04	13.57	16.8
13	IDD	1.87	9.45	22.6
14	XT	5.18	11.17	5.7
16a	FL	4.84	11.09	6.0
17	CMN	2.27	9.16	14.5

imides **7a–e** using the aromatic substituents parameters [21] π, MR, σ, $\mathcal{F}$ and $\mathcal{R}$ (see table VI). The cross correlation matrix (table VII) indicated that the best single parameter was σ, which implied that electronic effects associated with the core may be important to activity. This study resulted in equations 2a,b. All of these observations indicated a complex relationship between the composition of the core and activity.

$$-\log (EC_{50}) = 0.22 (\pm 0.10) \pi + 0.46 (\pm 0.11) \sigma - 0.89 (\pm 0.08) \quad (2a)$$

$n = 5$; $r = 0.968$; se = 0.090; $F = 14.942$; Prob > $F = 0.063$

$$-\log (EC_{50}) = 0.51 (\pm 0.15) \sigma - 0.90 (\pm 0.12) \quad (2b)$$

$n = 5$; $r = 0.787$; se = 0.135; $F = 11.107$; Prob > $F = 0.045$

Conclusion

Our AcCh release-enhancer program involved the synthesis and biological evaluation of over 1000 compounds, most of which were not included in this report. The results in this study are applicable to the other members of the series. The foregoing results suggest that some of the compounds discussed above significantly enhance the stimulated release of acetylcholine, and as such may have utility in the treatment of cognitive disorders and/or neurological function deficits and/or mood and mental disturbances in patients suffering from nervous system disorders like Alzheimer's disease. The results of the study showed that the ability to release acetylcholine in brain tissue could be correlated with the distance between the heteroatoms of the two pendant groups (Het-CH_2-C-CH_2-Het), and that this distance was best represented by the bis-4-pyridylmethyl groups (also see Wilkerson et al [3]). These heteroatoms function as HBAs (fig 7). For good activity, the core structure should have a lipophilic center and a HBA, which for this series was best represented by the carbonyl oxygen of anthrone. As can be seen in the overlap study with **1a** and **2a**

Table VI. Aromatic substituent constants for the homophthalimides **7a–e**.

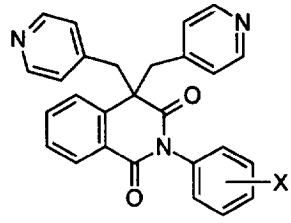

Compound	*X*	*–log (EC50)*	*π*	*MR*	*σ*	*$\mathcal{F}$*	*$\mathcal{R}$*
7a	H	–0.875	0.00	1.03	0.00	0.00	0.00
7b	2-F	–0.301	0.14	0.92	1.20	0.44	–0.34
7c	2-Br	–0.301	0.86	8.88	0.88	0.43	–0.17
7d	3-NO_2	–0.716	–0.28	7.36	0.71	0.67	0.16
7e	4-NO_2	–0.505	–0.28	7.36	0.78	0.67	0.16

Table VII. Cross correlation matrix for compounds **7a–e**.

	–log (EC50)	*π*	*MR*	*σ*	*$\mathcal{F}$*	*$\mathcal{R}$*
–log (EC_{50})	1.000	0.584	0.171	0.887	0.404	–0.654
π		1.000	0.521	0.234	–0.270	–0.656
MR			1.000	0.164	0.269	0.033
σ				1.000	0.677	–0.479
$\mathcal{F}$					1.000	0.319
$\mathcal{R}$						1.000

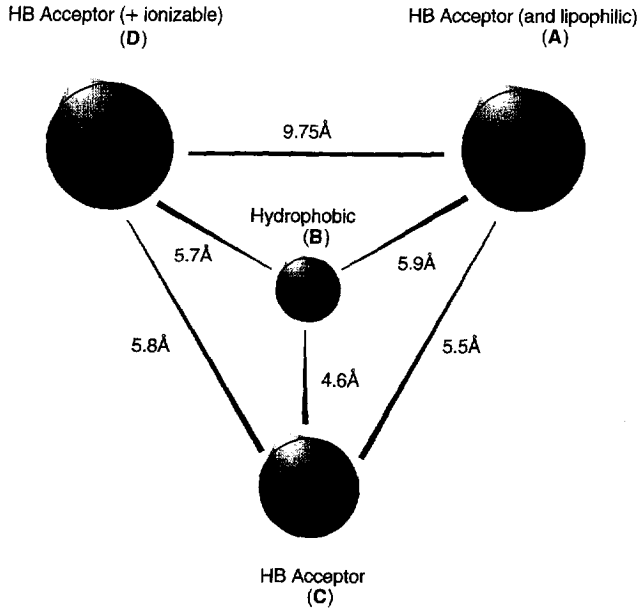

Fig 7. 'Free-hand' presentation of the proposed pharmacophores for the enhanced release of acetylcholine in the brain-slice preparation.

(fig 8), there is a distinct difference in the position of the proposed HB-acceptor associated with the core for the two molecules. With the overlap forced on the pyridyl nitrogen atoms and the methine carbons, the core portions were found in the same plane with some overlap of the hydrophobic region of the core. The distances between the HB-accepting carbonyl oxygen of **2a** and the carbonyl oxygen and lactam nitrogen of **1a** were found to be 2.8 Å and 2.0 Å respectively. In the overlap, the two carbonyls are orthogonal to one another. These SAR–QSAR and modeling data, in conjunction with an on-going investigation into descriptors for hydrogen bonding [25–28], should facilitate the identification of more potent AcCh release enhancers that may be totally different from the structures described above.

Experimental protocols

Synthesis

Melting points were determined with a Thomas–Hoover melting point apparatus and are uncorrected. The NMR spectra were recorded with a Varian-300S spectrometer, IR spectra were recorded with a Perkin Elmer 1650 FTIR spectrophotometer, UV spectra were obtained with a Cary 2415 spectrophotometer, and mass spectra (MS) were obtained using the Hewlett Packard HP5988A GC-MS system. Thin layer chromatography (TLC) was performed on silica gel plates.

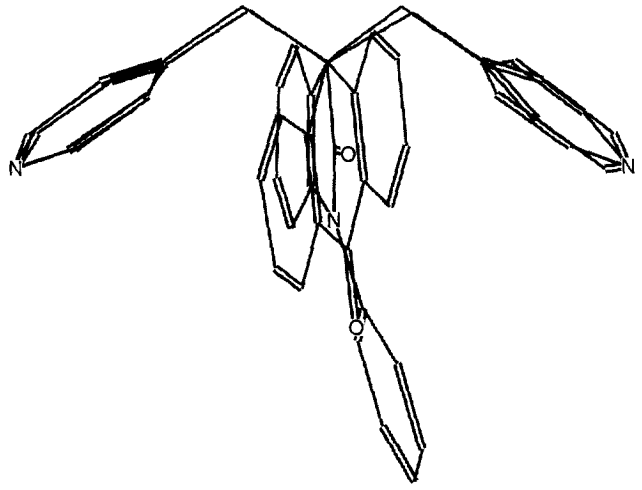

Fig 8. Overlap comparison for compounds **1a** and **2a**.

10,10-Bis-(4-pyridinylmethyl)-9(10H)-anthracenone ***2a***

A solution of 4-picolyl chloride hydrochloride (36.1 g, 0.22 mol) in 150 mL and 150 mL of benzene was treated with saturated $NaHCO_3$ until the aqueous phase was alkaline. The organic phase was washed with brine, dried over $MgSO_4$, filtered, and added to a mixture of 300 mL of benzene/water (1:1) containing anthrone (19.4 g, 0.1 mol) and 1 g tetrabutylammonium iodide. The mixture was stirred while treating dropwise over an hour with a solution of KOH (11.2 g, 0.2 mol) in 50 mL of water. After the addition of the base, the mixture was stirred at room temperature for 2 h and refluxed until no anthrone remained. The mixture was concentrated in vacuo to remove the benzene, and the mixture was diluted with 100 mL of CH_2Cl_2 and 300 mL of water. The organic phase was washed with water and brine, dried over $MgSO_4$, filtered, and concentrated in vacuo to give a dark brown gum. The gum was triturated with 200 mL *n*-BuCl, and the resulting crystals were collected by filtration, washed with *n*-BuCl, and dried to give the desired product in 62% (23.5 g) yield: mp 228.0–231 °C; ^1H NMR (300 MHz, $CDCl_3$ TMS), δ 3.73 (s, 4H, CH_2-Pyr), [6.19 (d, 4H), 7.46 (dd, 2H), 7.8 (dd, 2H), 8.0 (m, 6H), 8.13 (d, 2H), Ar]; IR (Nujol) 1657 (CO) cm^{-1}; UV-Vis (MeOH), λ_{max} 306 (3318), 273 (14415), 259 (21017) nm; MS (NH_3-DCI) *m/e* 377 (M + 1); Analysis calc for $C_{26}H_{20}N_2O$: C, 82.95; H, 5.36; N, 7.44; found: C, 82.94; H, 5.29; N, 7.34.

Enhanced acetylcholine release assay

Tissue preparation and release assays were performed as described previously by Nickolson et al [12]. Male Wistar rats (Charles River, 200–300 g) were euthanized by decapitation and the hippocampus was immediately dissected. The tissues were then chopped into 0.25 x 0.25 cm^2 squares using a McIlwain tissue chopper. Approximately 100 mg of the tissue slices were transferred to 10 mL of Krebs–Ringer solution, made up of 116 mM NaCl, 3 mM KCl, 1.3 mM $CaCl_2$, 1.2 mM KH_2PO_4, 1.2 mM Na_2SO_4, 25 mM $NaHCO_3$ and 11 mM glucose, and containing radiolabeled neurotransmitter precursor, 10 nmol choline chloride containing 20 μL of [^{3}H]-

choline chloride (80 Ci/mmol) for acetylcholine release; the preparation was allowed to incubate for 30 min under an atmosphere of O_2/CO_2 (95:5). After the incubation period, the slices were washed three times with fresh Krebs–Ringer buffer and aliquots of the slices (approx 5 mg) were transferred to perfusion chambers of a Brandel SF-20 superfusion apparatus. The slices were superfused (washed) with oxygenated Krebs–Ringer solution at a rate of 0.25 mL/min for 20 min before fractions of the effluent were taken. Hemicholinium-3 (10 μM) was added to the superfusion medium to inhibit reuptake of [^{3}H]-choline during the release assay. After the 20 min washout period, fractions were collected in 4 min intervals (1.0 mL fractions) directly into scintillation vials; at the end of the experiment, the chambers were emptied into scintillation vials and residual radioactivity was extracted from the slices in 100 μL of 1.0 N HCl. Scintillation cocktail was subsequently added to the vials, that were then assessed for radioactivity in a scintillation counter.

A total of 15 fractions were collected from each chamber during an experiment. Stimulated release was elicited by raising the KCl concentration to 20 mM (NaCl concentration adjusted to 100.2 mM) for a period of 4 min immediately before fraction 4 (S1), fraction 8 (S2), and fraction 13 (S3). The screening compound was introduced during fraction 5 (the lowest dose) and fraction 10 (the highest dose), with a 4 min washout in between. Fractional releases were calculated by dividing the radioactivity (dmp) found in each fraction by the total radioactivity in the tissue at the start of the experiment and were expressed as percentages. Stimulated release is defined as the fractional release found during K^+ stimulation minus the amount of fractional release found before and after stimulation.

References

1 12th International Symposium on Medicinal Chemistry; Basel, Switzerland; September 13–19, 1992; Abs OC-03.5

2 Francis PT, Palmer AM, Sims N et al (1985) *N Engl J Med* 313, 7–11

3 Wilkerson WW, Kergaye AA, Tam SW (1993) *J Med Chem* 36, 2899–2907

4 Fiske W, Saxton T, Martz R, Nibbelink D (1989) *Phamm Res* 6, S–34

5 Bryant WM, Huhn GF (1989) *US Patent* 4 806 651

6 DeNoble VJ, DeNoble KF, Spencer KR et al (1990) *Pharmacol Biochem Behav* 36, 957–961

7 Saletu B, Darragh A, Salmon P, Coen R (1989) *Br J Clin Pharmacol* 28, 1–16

8 Cook L, Nickolson V, Steinfels G, Rohrbach K, DeNoble V (1990) *Drug Dev Res* 19, 301–324

9 DeNoble VJ, DeNoble KF, Spencer KR (1991) *Brain Res Bull* 26, 817–820

10 Earl RA, Myers MJ, Johnson AL et al (1992) *Biomed Chem Lett* 2, 851–854

11 Gray JE, Peterman V, Nibbelink DW, Saxton TD, Fiske WD (1991) *Pharm Res* 8, 298S

12 Nickolson VJ, Tam SW, Myers MJ, Cook L (1990) *Drug Dev Res* 19, 285–300

13 Pieniaszek H, Xilinas M, Fiske W, Saxton T, Garner D, Kim Y (1989) *Pharm Res* 6, 35S

14 Rohrbach K, Cook L (1990) *FESEB* 4, 1109A

15 Saletu B, Darragh A, Breuel HP, Herrmann W, Salmon P, Coen R (1991) *Human Psychopharmacol* 6, 267–275

16 Tam SW, Rominger D, Nickolson VJ (1991) *Mol Pharmacol* 40, 16–21

17 Myers MJ, Nickolson VJ (1988) *US Patent* 4 760 083

18 Crapps EC (1993) *US Patent* 5 185 447

19 Pierce ME, Huhn GF, Jensen JH, Sigvardson KW, Islam Q, Xing Y (1994) *J Heterocycl Chem* 31, 17–23

20 Wilkerson WW (1994) *US Patent* 5 278 162

21 Hansch C, Leo A (1979) In: *Substituent Constants for Correlation Analysis in Chemistry and Biology*. John Wiley and Sons, New York

22 Brown KL, Fullerton TJ (1980) *Acta Crystallogr* Sect B 36, 3199

23 Topliss JG, Edwards RP (1979) *J Med Chem* 22, 1238–1244

24 Topliss JG, Costello RJ (1972) *J Med Chem* 15, 1066–1068

25 Wade RC, Goodford PJ (1993) *J Med Chem* 36, 148–156

26 Murray JS, Ranganathan S, Politzer P (1991) *J Org Chem* 56, 3734–3737

27 Neder KM, Whitlock Jr HW (1990) *J Am Chem Soc* 112, 9412–9414

28 Kamlet MJ, Abboud JLM, Abraham MH, Taft RW (1983) *J Org Chem* 48, 2877–2887